Hydroxyapatite of natural origin - zirconia composites, preparation and reactions within the system

Jadwiga Brzezińska-Miecznik, Krzysztof Haberko, Mirosław M. Bućko, Grzegorz Grabowski, Maciej Sitarz[*]

AGH-University of Science and Technology, Faculty of Materials Science and Ceramics, Al. Mickiewicza 30, 30-059 Krakow, Poland

Abstract

The effect of 5 and 10 vol.% addition of zirconia (3Y-TOSOH) to hydroxyapatite of natural origin was investigated. The hydroxyapatite (HAp) material was extracted from the bovine bones by treatment under hydrothermal conditions with distilled water. The pure HAp and HAp-ZrO_2 composites were manufactured by pressureless sintering and hot pressing. The reactions taking place in these systems were observed using the X-ray diffraction, infrared spectroscopy and dilatometric observations. It was confirmed that the extent of the reactions was essentially dependent on the heat treatment method. Under the hot pressing conditions dense samples containing high fraction of unreacted HAp could be prepared at 1200 °C. Mechanical properties of the pure HAp and HAp-ZrO_2 composites were also investigated. Zirconia inclusions lead to the increased strength, hardness and fracture toughness of the composites compared to the pure HAp polycrystalline materials.

Keywords: natural hydroxyapatite, zirconia, composites, reactions, sintering

I. Introduction

Biocompatibility, bioactivity and the lack of carcinogenic properties promote hydroxyapatite (HAp) as a bone implant material. Hydroxyapatite of natural origin is essentially different from the synthetic material. It differs from the stoichiometric Ca/P ratio (1.67) and contains CO_3^{-2} groups. Moreover, in the HAp of natural origin some other cations are present (Na, Mg, etc.). It can be extracted from animal bones by three techniques: i) the bone calcination [1–7], ii) the bone treatment with sodium hydroxide [4,5,8–11] at elevated temperatures and iii) the bone treatment with water or sodium hydroxide under hydrothermal conditions [5,12].

The pure HAp polycrystalline materials show poor mechanical properties [13]: low strength and low fracture toughness. That is why different inorganic additives have been introduced to the HAp matrix in order to improve these properties. Among others, zirconia [6,12,14–19], alumina [6,20], titania [6,19], yttria [19], Ti_3SiC_2 [21] and zinc oxide [7] should be mentioned. Zirconia is characterized by excellent biocompatibility and durability in the physiological environment [22]. The zirconia inclusions make densification during sintering less effective than in the case of the pure HAp material [12,14]. This is due to the effect of inclusions as such and due to the reaction of zirconia and HAp matrix. It was found [6,12,14–19] that this reaction leads to the HAp decomposition resulting in formation of β-TCP, a solid solution of CaO in ZrO_2 and the water vapour emission caused by HAp dehydroxylation. Water vapour leads to the pore formation which was observed both during pressureless sintering [15,18] and hot pressing [16].

The aim of the present work was to investigate the HAp-ZrO_2 composites, manufactured by pressureless sintering and hot pressing. Zirconia (TOSOH) powder containing 3 mol% Y_2O_3 was used as source of ZrO_2 and HAp component was extracted from the bovine bones by their treatment with distilled water under hydrothermal conditions.

II. Experimental

2.1. Materials

Hydroxyapatite was obtained from the long bovine

[*]Corresponding author: tel: +48 6172395,
fax: +48 126337161, e-mail: *msitarz@agh.edu.pl*

bones. 3-year-old animals were selected. The bone ends were cut off and spongy parts were removed together with marrow. The bones prepared in this way were hydrothermally treated in an autoclave at 220 °C for 10 h in distilled water. Then the material was washed several times with hot distilled water and dried at 110 °C. Precursor of zirconia was ZrO_2 TOSOH powder with 3 mol% Y_2O_3 (3YTZP) further denoted as ZrO_2.

Homogenization of zirconia and HAp powders was performed in a ball mill using the zirconia grinding media of 10 mm diameter in propanol for 5 h. The homogenized composite powders were dried at 120 °C. Two compositions with different ZrO_2 contents of 9.1 and 14.5 wt.% were prepared, which corresponds to HAp-5Z and HAp-10Z samples containing 5 and 10 vol.% of ZrO_2, respectively (assuming zirconia density to be 6.01 g/cm^3 and HAp density to be 3.16 g/cm^3). The uniaxial compaction of the powders under 35 MPa with the subsequent isostatic repressing under 300 MPa allowed us to prepare cylindrical samples of 20 mm diameter and about 3 mm thickness. Such samples underwent pressureless sintering in air atmosphere at 1400 °C and 1500 °C, with the rate of temperature increase 2 °C/min up to 600 °C and then 5 °C/min. The soaking time at the final temperature was 1 h. The sample shrinkage was followed using the NETZSCH dilatometer (Dil 402 C) up to 1500 °C with the rate of temperature increase of 5 °C/min. Since the pressureless sintering did not allow us to get the state of sufficient densification the hot pressing was also applied. It was performed by means of the Thermal Technology HP50-7010G equipment. The temperature of 1200 °C with 30 min. soaking time, the temperature increase rate of 15 °C/min and the pressure of 25 MPa were used. The process was performed in Ar atmosphere.

2.2. Methods

The chemical composition of hydroxyapatite was determined using the X-ray fluorescence method (spectrometer WDXRF Axios Max PANanalytical). The Omnian package (Panalytical) was used for the standardless analysis of all types of samples. The standardless analysis, in nutshell is based only on the initial calibration with pure element standards and further deconvolution of spectra that allows the determination of all elements in whatever sample matrix. Standardless method combines: i) matrix effect calculation using a FP algorithm solving the Sherman equation (intensities) and ii) instrumental sensitivity determination by standards measurements (relationship between intensity and elemental mass). As instrumental sensitivity is determined once, this allows analysis of any sample without a need of any matrix-matched calibration standards leading to so-called "standardless analysis".

The infrared spectroscopy (MIR) was used to characterize the hydrothermally treated hydroxyapatite (BIO-RAD FT6000). The specific surface area of the powders was determined by the nitrogen adsorption with the BET isotherm (Nova 1200e, Quantachrome Instruments). Morphology of the starting HAp powder was observed under transmission electron microscope (JEOL-JEM 1011). The phase composition of the powders and sintered materials was characterized by the X-ray diffraction applying CuKα irradiation (X'PERT PRO). The quantitative composition was determined by the Rietveld method. The DTA/TG combined with the chemical analysis (Mass Spectrometer QMD 300 Thermostar) of gases emitted by the hydroxyapatite was useful in its characterization. The effects of gasses emission and DTA analysis were related to 1 mg of sample. Dilatometric measurements (NETSCH DIL 402C) allowed us to follow shrinkage of the powder compacts *vs* temperature.

The Archimedes method was used to measure the density of the samples. The SEM observations (Nova Nano SEM 200) were applied to evaluate the microstructure of the sintered materials. Hardness and fracture toughness were determined by indentation with the Vickers pyramid (FV700Future Tech Corp, Japan). The Palmqvist cracks model [23] was used to calculate fracture toughness. Bending strength was determined by the two-axis bending (Zwick/Roell Z150) of the disc samples supported on 3 balls (ISO 6872:2008E).

III. Results and discussion

The chemical analysis of the starting hydroxyapatite powder shows that this is not a stoichiometric material. Thus, Ca/P molar ratio equals to 1.76 (as compared to 1.67 in the stoichiometric material) and, moreover, it contains Mg (0.72 wt.%) and Na (0.51 wt.%). Morphology of the starting HAp powder is presented in Fig. 1. Plate-like morphology of the powder is evident.

According to the ICDD cards, X-ray diffraction analysis (Fig. 2) indicates that the material extracted from the bone corresponds to hydroxyapatite. Its specific surface area corresponds to 59.3 m^2/g and is much higher than that of the zirconia powder (15.0 m^2/g). X-ray diffraction shows that ZrO_2 powder contains 70.3 wt.% of the tetragonal phase and 29.7 wt.% of the monoclinic phase.
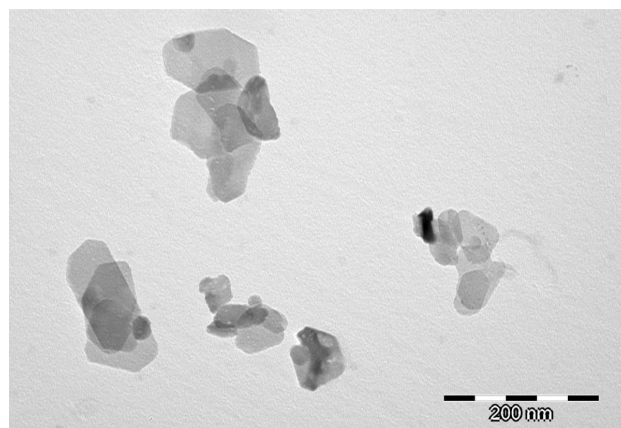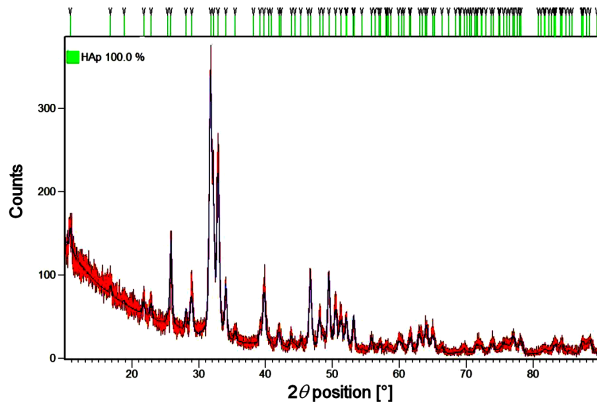

Figure 1. TEM of the starting HAp powder

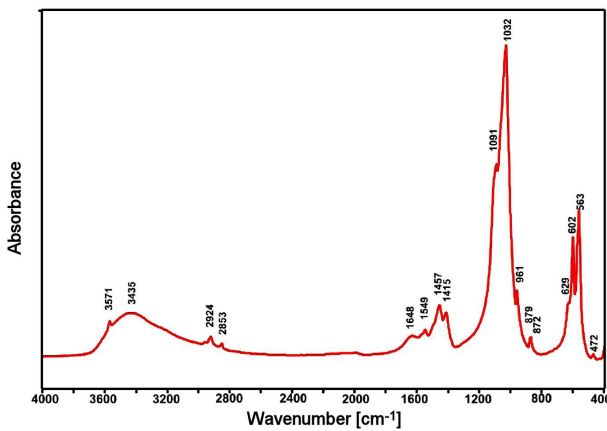**Figure 2. XRD pattern of the hydrothermally extracted HAp powder**

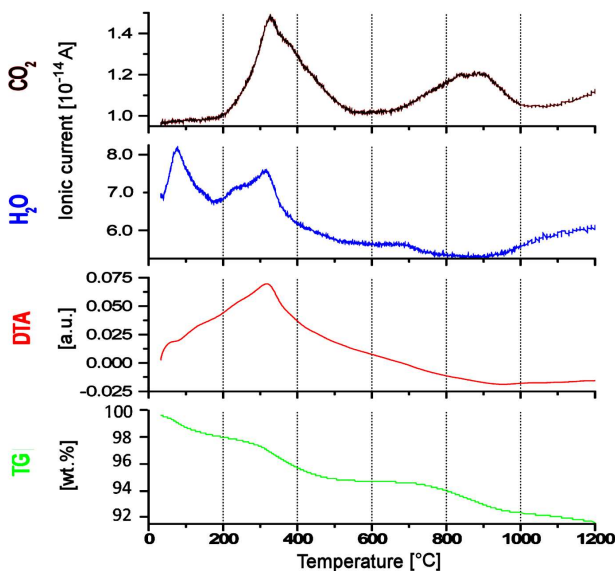**Figure 3. MIR spectrum of the hydrothermally extracted HAp powder**

Figure 4. DTA/TG curves and analysis of the H_2O and CO_2 emitted by the hydrothermally extracted HAp powder

Some further information was delivered from the IR spectra (Fig. 3). The absorption bands at $879\,cm^{-1}$, $1415\,cm^{-1}$, $1457\,cm^{-1}$ and $1549\,cm^{-1}$ indicate the presence of the CO_3^{-2} groups in the material of natural ori-

gin. The absorption bands at $629\,cm^{-1}$ and $3571\,cm^{-1}$ should be attributed to the hydroxyapatite OH^- groups. The remaining bands at $1091\,cm^{-1}$ and $1032\,cm^{-1}$ originate from doubly degenerated asymmetric stretching vibrations v_3 P−O and symmetric stretching vibrations of v_1 P−O corresponds to $961\,cm^{-1}$. The absorption maxima at $602\,cm^{-1}$ and $563\,cm^{-1}$ can be attributed to the triply degenerated bending vibrations v_4 O−P−O.

Figure 4 demonstrates DTA/TG curves of the hydrothermally extracted HAp powder. At low temperatures (about $100\,°C$) water molecules, most probably adsorbed on the particle surfaces is emitted. At higher temperatures (above $200\,°C$) we observe the emission of H_2O and CO_2 accompanied by the exothermic effect and mass decrease. This should presumably be related to the oxidation of the rest of organic matter remained in the material after its hydrothermal treatment. At a higher temperature intensive emission of CO_2 (about $800\,°C$) and H_2O (above $1000\,°C$) occurs.

The dilatometric curves illustrate shrinkage of the pure HAp powder compact and HAp-5Z and HAp-10Z mixtures (Fig. 5). In the case of the pure HAp powder compact a "smooth" shrinkage curve occurs. The shrinkage terminates at about $1100\,°C$. But in the case of the composites shrinkage ended at much higher temperatures. Most probably this phenomenon should be attributed to the interfering effect of the reaction between zirconia and decomposed HAp (CaO + β-TCP). The reaction is manifested by the shrinkage slowdown, which is more distinct in HAp-10Z than HAp-5Z composite, due to the higher zirconia content in the former material.

The reaction between zirconia and decomposed HAp is also proved by measurements of the phase composition of the pressureless sintered and the hot pressed materials (Table 1). The investigation was performed by X-ray diffraction of the sample surfaces as well as the samples powdered in a mortar. Pressureless sintering leads to the composite materials whose phase composition differs from those subjected to hot pressing procedure. In the case of the pressureless sintered materials, traces of HAp are present on the sample surface only in the HAp-5Z composite heat treated at $1400\,°C$. In other cases the entire HAp phase disappears. It is worth noting that phase composition of the HAp-10Z samples pressureless sintered and hot pressed at $1200\,°C$ are similar, but pressureless sintering does not lead to high densification as hot pressing does. In the former case an increase of reaction degree with sintering temperature is evident, but there is only slight increase of sample density (Tables 2 and 3).

The hot pressing leads to the composites of much higher HAp content. This phenomenon can be attributed to the lower heat treatment temperature in the case of the hot pressed materials. Another important factor originates from the totally different densification conditions. This is related to the fact that the process is performed in a closed vessel of the graphite die. Under such conditions the escape of gases (H_2O, CO_2), which results
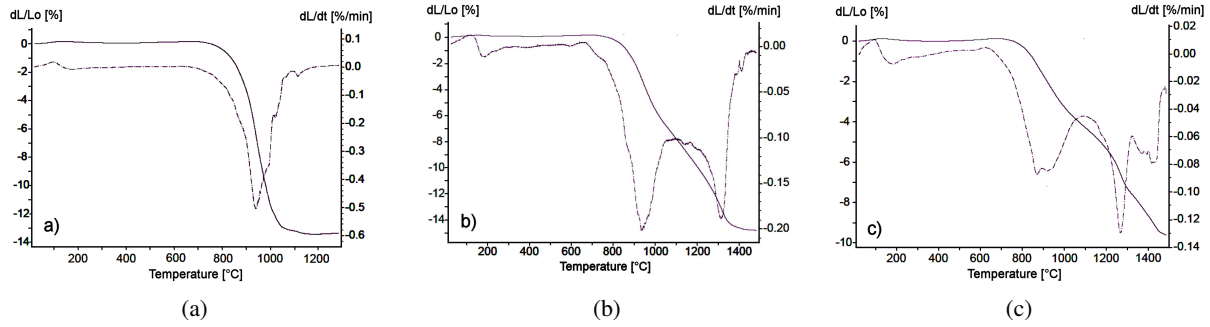
Figure 5. Dilatometric curves of: a) pure HAp powder compact, b) HAp-5Z powder compact and c) HAp-10Z powder compact
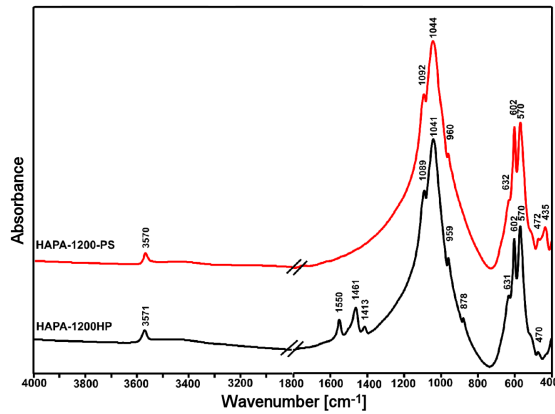

Figure 6. MIR spectra of pure HAp material pressureless sintered (PS) and hot pressed (HP)

from the HAp thermal decomposition and the reaction between HAp and ZrO_2 is limited. This is proved by the lower degree of HAp decomposition in the sample volume (represented in this case by the powdered material), than on its surface. The decomposition of HAp leads to the formation of β-TCP. Since the extension of the HAp decomposition in the hot pressed material is lower, a lower amount of β-TCP in the hot pressed processed material can be observed.

The data in Table 1 indicate the occurrence of the cubic zirconia solid solution, most probably due to the saturation of this oxide with CaO. Free CaO results

from the decomposition of HAp at high temperature and its reaction with zirconia. When the concentration of CaO in ZrO_2 exceeds a certain level, calcium zirconate ($CaZrO_3$) appears. Since the degree of reaction under the hot pressing conditions is low, an insufficient amount of CaO becomes available. That is why $CaZrO_3$ is not observed in the hot pressed composites. An open question appears: what happens with Y_2O_3 present in the starting TOSOH powder. Most probably it retains in zirconia and/or enters the HAp structure. We observed the latter possibility in an unpublished study on sintering of the HAp-Y_2O_3 mixture.

The investigations performed with the powdered materials are also shown in Table 1. The X-ray diffraction patterns show hydroxyapatite as the only phase. However, the IR spectroscopy indicates that under the pressureless sintering conditions carbonate groups disappear from the material, but the hot pressing process leads to the body with the carbonate groups retained in the material structure (Fig. 6). In each case hydroxyapatite structure is still preserved no matter of heat treatment conditions.

The spectroscopic measurements (MIR) of the powdered composite samples for both the pressureless sintered and the hot pressed samples are presented in Fig. 7. The hot-pressed materials show the existence of the CO_3^{-2} and OH^- groups. The former ones are presented by the absorption bands at about 880, 1410, 1460 and

Table 1. Phase composition of the pressureless sintered materials and hot pressed samples (measured on the surface or with powdered sample)

Sample	Phase composition [wt.%]					Phase
	Pressureless sintering			Hot pressing		
	1200 °C (surface)	1400 °C (surface)	1500 °C (surface)	1200 °C (surface)	1200 °C (ground sample)	
HAp	100	-	-	100	100	HAp
HAp-5Z	-	6	0	81.7	84.6	HAp
	-	82.7	83.1	7.7	5.7	β-TCP
	-	0	0	10.6	9.7	c-ZrO_2
	-	11.3	16.9	0	0	$CaZrO_3$
HAp-10Z	61.5	0	0	60.5	73.3	HAp
	19.6	77.3	75.2	16.3	8.2	β-TCP
	17.3	6.4	5.7	23.2	18.2	c-ZrO_2
	1.6	16.2	19.1	0	0	$CaZrO_3$

Table 2. Apparent densities of the pressureless sintered and hot pressed samples

Sample	Apparent density[a] [g/cm^3]			
	1200 °C PS	1400 °C PS	1500 °C PS	1200 °C HP
HAp	3.11±0.01	-	-	3.08±0.02
HAp-5Z	-	3.19±0.07	3.16±0.02	3.28±0.02
HAp-10Z	2.23±0.02	2.57±0.02	2.72±0.02	3.37±0.05

[a]Confidence interval at confidence level of 0.95

Table 3. Open porosities of the pressureless sintered and hot pressed samples

Sample	Open porosity[a] [%]			
	1200 °C PS	1400 °C PS	1500 °C PS	1200 °C HP
HAp	0	-	-	0
HAp-5Z	-	0.6±0.1	1.8±0.02	0
HAp-10Z	34.4±0.02	22.6±1.6	15.9±0.8	0

[a]Confidence interval at confidence level of 0.95

1550 cm^{-1}. The existence of the hydroxyl groups is confirmed by absorption bands at about 3570 and 632 cm^{-1}. We can conclude that under the hot pressing conditions none or a very limited decomposition of HAp occurs in the material volume as it is indicated by a small shoulder at about 975 cm^{-1} in the HAp-10Z material (indicated by an arrow in Fig. 7b).

A lower ZrO_2 content leads to the higher densification of the pressureless sintered materials, but presence of open porosity is also characteristic of these materials. In the case of the higher zirconia content (10 vol.%), the pressureless sintered samples are far from fully dense materials as it is demonstrated by a relatively high volume fraction of the open porosity. Essentially higher densification without open porosity was observed (Tables 2 and 3) in the case of hot-pressed material compared to the pressureless sintered one. The results presented in Tables 2 and 3 demonstrate also essentially higher densification of the pressureless sintered material with no zirconia additive.

The microstructures of the hot pressed and pressureless sintered composite materials are shown in Fig. 8. The essential difference in their densification is evident and agrees well with the data given in Tables 2 and 3. It is also evident that zirconia additive restrains grain growth of the HAp matrix.

Table 4 shows only mechanical properties of the hot pressed composite materials as pressureless sintered composites do not reach high enough density. However, pressureless sintering results in high density of the pure HAp powder compacts. Thus, their mechanical properties are shown also in Table 4 together with the properties of the hot pressed pure HAp compacts. Hot pressing of the pure HAp powder improves only slightly bending strength and hardness of the resulting polycrystalline materials. However, strength, hardness and fracture toughness of composites are higher than those of the pure HAp materials, although reduced content of hydroxyapatite occurs in composites due to the matrix/zirconia reaction (Table 3).
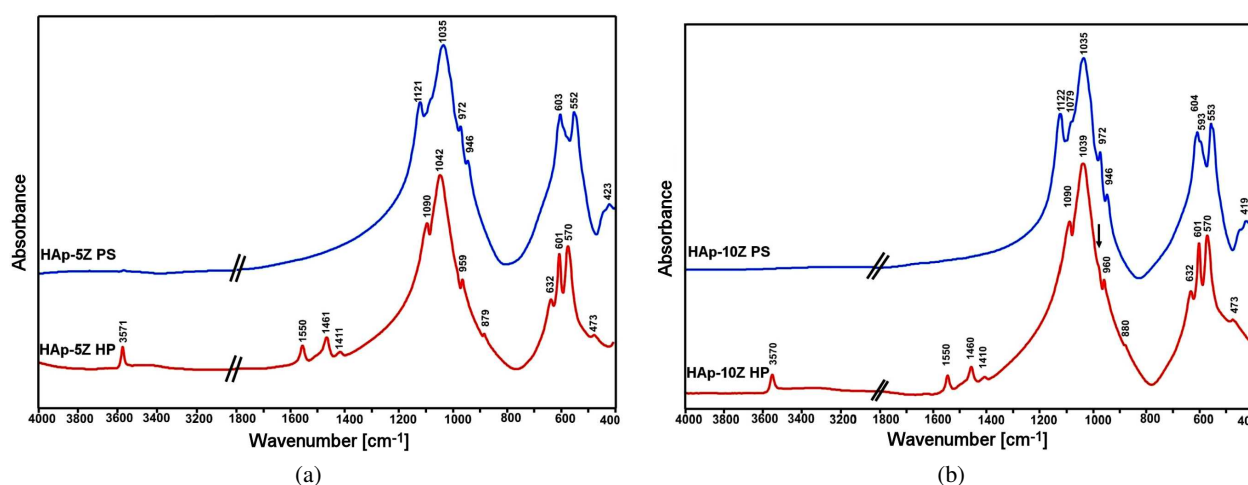

(a)

(b)

Figure 7. MIR spectra of: a) HAp-5Z and b) HAp-10Z composites - pressureless sintered (PS) at 1400 °C and hot pressed (HP) at 1200 °C
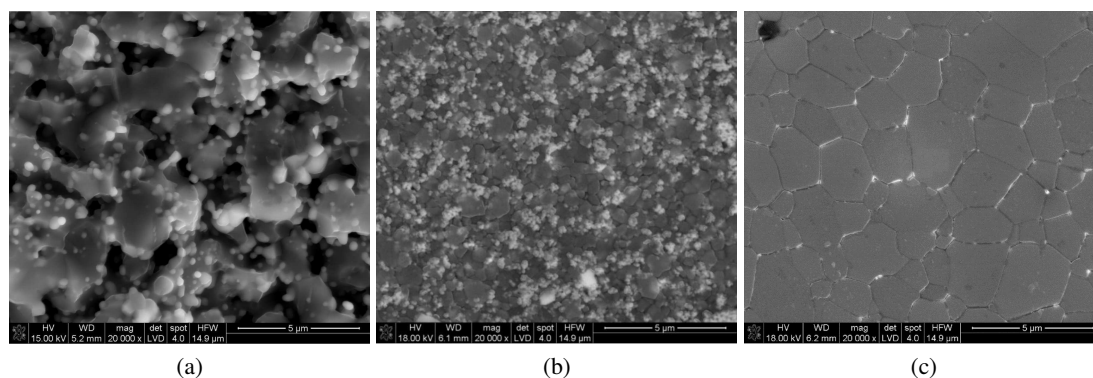
(a)　　　　　　　　　　　(b)　　　　　　　　　　　(c)

Figure 8. Microstructure of the pressureless sintered and the hot pressed materials: a) HAp-10Z composite - pressureless sintered at 1400 °C, b) hot pressed at 1200 °C HAp-10Z composite and c) hot pressed at 1200 °C pure HAp

Table 4. Bending strength (σ), hardness (HV) and fracture toughness (K_{Ic}) of the materials

Sample	Sintering conditions	HV [GPa]	σ [MPa]	K_{Ic} [MPa m$^{1/2}$]
HAp	PS 1200 °C - 2 h	4.6±0.3	60±20	0.6±0.1
HAp	HP 1200 °C - 0.5 h	4.9±0.2	105±22	0.5±0.1
HAp-5Z	HP 1200 °C - 0.5 h	5.7±0.5	149±27	0.7±0.1
HAp-10Z	HP 1200 °C - 0.5 h	5.6±0.2	134±25	1.0±0.2

IV. Conclusions

Presented data indicate that bovine bones treatment with distilled water under hydrothermal conditions at 220 °C allowed us to extract hydroxyapatite with interesting properties. It was demonstrated that this is not a stoichiometric material (Ca/P-1.76) and contains some CO_3^{-2} groups. No traces of decomposition of this material at elevated temperatures under pressureless nor hot pressing conditions occur. The dilatometric investigation indicated that the reaction between zirconia and HAp results in slowing down the shrinkage. It is accompanied by the emission of H_2O and CO_2 from the system. This reaction and HAp decomposition is essentially less advanced under hot pressing conditions and leads to a much higher densification of the materials. In the hot-pressed composites the CO_3^{-2} and OH^- groups are retained in the HAp structure. This is most probably due to the limited possibility of H_2O and CO_2 emission from the tight graphite die. It was also confirmed that the higher zirconia content in the composite material leads to the higher degree of the HAp decomposition. Under pressureless conditions, complete or almost complete HAp decomposition occurs. Zirconia additive improves mechanical properties of the materials compared to the pure polycrystalline HAp ceramics.

References

1. C.Y. Ooi, M. Hamdi, S. Ramesh, "Preparation of hydroxyapatite produced by annealing of bovine bone", *Ceram. Int.*, **33** (2007) 1171–1177.
2. A. Sobczak-Kupiec, Z. Wzorek, "The influence of calcination parameters on free calcium oxide content in natural hydroxyapatite", *Ceram. Int.*, **38** (2012) 641–664.
3. M. Figueiredo, A. Fernando, G. Martins, J. Freitas, F. Judas, H. Figueiredo, "Effect on the composition and microstructure of hydroxyapatite derived from human and animal bone", *Ceram. Int.*, **36** (2010) 2383–2393.
4. J. Venkatesan, Z.J. Qian, B.M. Ryu, N.V. Thomas, S.K. Kim, "A comparative study of thermal calcination and an alkaline hydrolysis method in the isolation of hydroxyapatite from Thunnus obesus bone", *Biomed. Mater.*, **6** (2011) 035003.
5. N.A.M. Barakat, K.A. Khalil, F.A. Sheikh, A.M. Omran, B. Gaihre, S.M. Khil, H.Y. Kim, "Physiochemical characterizations of hydroxyapatite extracted from bovine bones by three different methods: extraction of biologically desirable HAp", *Mater. Sci. Eng. C*, **28** (2008) 1381–1387.
6. F. Mezahi, A Harabi, S. Zouai, S Achour, D Bernache-Assollant, "Effect of stabilized ZrO_2, Al_2O_3 and TiO_2 on sintering hydroxyapatite", *Mater. Sci. Forum*, **492-493** (2005) 241–248.
7. O. Gunduz, E.M. Erkan, S. Dagliar, S. Agathopoulos, F.N. Oktar, "Composites of bovine hydroxyapatite (BHA) and ZnO", *J. Mater. Sci.*, **43** (2008) 2536–2540.
8. J. Brzezińska-Miecznik, K. Haberko, M. Sitarz, M.M. Bućko, B. Macherzyńska, "Hydroxyapatite from animals bone - Extraction and properties", *Ceram. Int.*, **41** (2015) 4841–4846.
9. K. Haberko, M.M. Bućko, J. Brzezińska-Miecznik,

M. Haberko, W. Mozgawa, T. Panz, A. Pyda, J. Zarębski, "Natural hydroxyapatite - its behaviour during heat treatment", *J. Eur. Ceram. Soc.*, **26** (2006) 537–542.

10. K. Haberko, M.M Bućko, W. Mozgawa, A. Pyda, J. Brzezińska-Miecznik, J. Carpentier, "Behaviour of bone origin hydroxyapatite at elevated temperatures and in O_2 and CO_2 atmospheres", *Ceram. Int.*, **35** (2009) 2537–2540.

11. Ş. Gören, H. Gökbayrak, S. Altintaş, "Production of hydroxyapatite from animal bone", *Eng. Mater.*, **264-268** (2004) 1949–1952.

12. J. Brzezińska-Miecznik, B. Macherzyńska, R. Lach, B. Nowak, "The effect of calcination and zirconia addition on HAp hot pressed materials", *Ceram. Int.*, **40** (2014) 15815–15819.

13. Ch. Benaqqaa, J. Chevalier, M. Saadaoui, G. Fantozzi, "Slow crack growth behaviour of hydroxyapatite ceramics", *Biomaterials*, **26** (2005) 6106–6112.

14. W. Pyda, A. Ślósarczyk, M. Haberko, Z. Paszkiewicz, A. Rapacz-Kmita, A. Pyda, "Effect of chemical composition and morphology of zirconia particles on properties of HAp-zirconia particulate composites", *Key Eng. Mater.*, **206-213** (2002) 1567–1570.

15. Z. Evis, "Reaction in hydroxylapatite–zirconia composites", *Ceram. Int.*, **339** (2007) 987–991.

16. Z. Evis, R.H. Doremus, "Hot pressed hydroxylapatite/monoclinic zirconia composites with improved mechanical properties", *J. Mater. Sci.*, **42** (2007) 2426–2431.

17. E. Adolfsson, P. Alberius-Henning, L. Hermansson, "Phase analysis and thermal stability of hot isostatically pressed", *J. Am. Ceram. Soc.*, **83** (2000) 2798–2802.

18. K.A. Khail, S.W. Kim, H.Y. Kim, "Consolidation and mechanical properties of nanostructured hydroxyapatite-(ZrO_2+3 mol% Y_2O_3) - bioceramics by high frequency induction heat sintering", *Mater. Sci. Eng. A*, **456** (2007) 368–372.

19. M.A. Auger, B. Savoini, A. Munoz, T. Leguey, M.A. Monge, R. Pareja, J. Victoria, "Mechanical characteristics of porous hydroxyapatite/oxide produced by post-sintering hot isostatic pressing", *Ceram. Int.*, **35** (2009) 2373–2380.

20. J. Li, B. Fartash, L. Hermanson, "Hydroxyapatite-alumina composites and bone-bonding", *Biomaterials*, **16** (1995) 417–422.

21. S.L. Shi, W. Pan, M.H. Fang, Z.Y. Fang, "Reinforcement of hydroxyapatite bioceramic by addition of Ti_3SiC_2", *J. Am. Ceram. Soc.*, **89** (2006) 743–745.

22. C. Piconi, G. Maccauro, "Zirconia as a ceramic biomaterial", *Biomaterials*, **20** (1999) 1–25.

23. K. Niihara, "A fracture mechanics analysis indentation Palmqvist crack in ceramics", *J. Mater. Sci. Lett.*, **2** (1983) 221–223.